

EPJ B

Condensed Matter
and Complex Systems

EPJ.org

your physics journal

Eur. Phys. J. B **82**, 63–67 (2011)

DOI: 10.1140/epjb/e2011-20202-3

Wigner crystal in snaked nanochannels

O.V. Zhirov and D.L. Shepelyansky



Wigner crystal in snaked nanochannels

O.V. Zhirov¹ and D.L. Shepelyansky^{2,a}

¹ Budker Institute of Nuclear Physics, 630090 Novosibirsk, Russia

² Laboratoire de Physique Théorique du CNRS (IRSAMC), Université de Toulouse, UPS, 31062 Toulouse, France

Received 15 March 2011 / Received in final form 1st May 2011

Published online 29 June 2011 – © EDP Sciences, Società Italiana di Fisica, Springer-Verlag 2011

Abstract. We study the properties of a Wigner crystal in snaked nanochannels and show that they are characterized by a conducting sliding phase at low charge densities and an insulating pinned phase above a critical charge density. The transition between these phases has a devil's staircase structure typical for the Aubry transition in dynamical maps and the Frenkel-Kontorova model. We discuss the implications of this phenomenon for charge density waves in quasi-one-dimensional organic conductors and for supercapacitors in nanopore materials.

1 Introduction

The Wigner crystal [1] appears in a great variety of physical systems including electrons in two-dimensional semiconductor samples and one-dimensional (1D) nanowires (see review [2] and Refs. therein), electrons on a surface of liquid helium [3], cold ions in radio-frequency traps [4] and dusty plasma in laboratory or in space [5]. Effects of Coulomb interactions are clearly seen experimentally in nanowires and carbon nanotubes [6–10]. Also interaction effects for electrons in microchannels on a surface of liquid helium have been recently observed experimentally [11]. In view of this remarkable progress it is interesting to investigate sliding and conducting properties of the Wigner crystal in wiggled or snaked nanochannels. The interest to such studies goes back to the Little suggestion [12,13] on electron conduction in long spine conjugated polymers where he proposed an approach for synthesizing organic superconductors. A modern overview discussion of this important suggestion is given in [14]. A schematic image of electron transport in such organic molecules is shown in Figure 1a. According to this picture long molecules form wiggling channels which in principle can support electron transport along them. However, the Coulomb interactions between electrons are rather strong at such small scales and thus it is not obvious under what conditions a sliding of Wigner crystal along such channels is possible. This problem is related to the conduction properties of charge density waves (CDW) (see e.g. reviews [14,15]). To study this phenomenon we choose a simple model of 1D snaked channel shown in Figure 1b. There is no potential gradient along the channel but the channel walls are assumed to be very high so that electrons can move only along the channel.

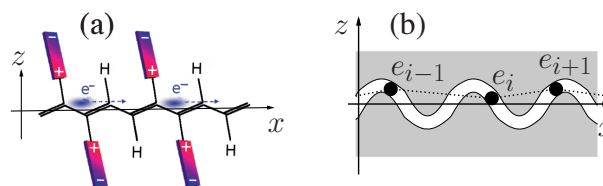


Fig. 1. (Color online) (a) A schematic image of the Little suggestion for electron transport in organic molecules (after [12–14]). (b) A schematic image of electron Wigner crystal with charges e_i (points) sliding in a snaked sinusoidal nanochannel, dashed lines show force directions between nearby electrons.

In addition, the properties of Wigner crystal in snaked nanochannels are also useful for the understanding mechanisms of charge storage in electrochemical capacitors, or supercapacitors, which start to have important industrial applications [16,17]. In these systems, charged ions are stored in nanopores at the surface of the carbon-activated material which has enormously large capacitance C going beyond the meanfield values given by the Helmholtz theory [18,19]. At nanoscale the wiggling of pores is definitely present and makes our studies rather timely.

Due to sinusoidal channel wiggling the Wigner crystal moves in a certain effective periodic potential. The case of a sliding 1D Wigner crystal in a periodic energy potential was analyzed in [20] having in mind an example of ion chains in optical lattices. It was shown there that this problem can be locally reduced to the Frenkel-Kontorova model for a particle spring chain in a periodic potential [21] with particle positions described by the Chirikov standard map [22]. For a small amplitude of periodic potential the Wigner crystal with an incommensurate ion density can slide in an optical lattice but above a certain critical amplitude of potential the crystal is pinned

^a e-mail: dima@irsamc.ups-tlse.fr

by the lattice due to the Aubry analyticity breaking transition [23]. In the pinned phase the phonon spectrum has a gap for long wave excitations so that this regime corresponds to an insulating phase. This situation corresponds to a dynamical spin glass phase with exponentially many stable classical configurations being exponentially close to a ground state at a fixed electron density [20]. The Frenkel-Kontorova model is characterized by similar classical and quantum properties [24,25]. The presence of many energy configurations being exponentially close in energy to the ground state is a characteristic feature of spin glass systems (see e.g. [26]) where disorder is intrinsically present e.g. in spin couplings. In contrast, models of the Frenkel-Kontorova type have no intrinsic disorder being characterized by a well defined rather simple Hamiltonian. However, due to nonlinearity of interactions they have exponentially many quasi-stable configurations that leads to very long relaxation times. As a result they have been called dynamical spin glass [20,24,25]. Akin to dynamical chaos, the word *dynamical* means that randomness appears due to dynamical deterministic equations and not due to external imposed disorder.

At sufficiently large values of effective Planck constant a quantum instanton tunneling between these quasidegenerate configurations leads to a zero-temperature quantum phase transition at which point the quantum Wigner crystal becomes conducting [20]. In the following we show that the main elements of this physical picture remain valid for the Wigner crystal in snaked nanochannels which are however characterized by enormously sharp changes of conducting properties. We also show that the sliding conditions for the Wigner snake in a wiggled nanochannel have striking differences compared to the usual case of the Frenkel-Kontorova model.

In Section 2 we provide the description of the model and present the numerical results. The discussion is given in Section 3.

2 Model description and numerical results

We start our analysis from the case of classical electrons with Coulomb interactions moving in a snaked nanochannel shown in Figure 1b. In this case the total system energy E is given by a sum over all Coulomb interactions. Due to strong nonlinearity of the system the minimal energy configurations should be found numerically using the methods described in [20,23–25]. We take a finite number of electrons N for L periods of a channel of finite length. In numerical simulations we put the channel on a cylindrical surface in 3D with electron coordinates being $x_i = L \sin(s_i/L)$, $y_i = L \cos(s_i/L)$, $z = a \sin(s_i)$ where s_i is coordinate along channel for electron i . Thus the channel, filled by N electrons, wiggles in the z -direction making L periodic oscillations along cylinder of radius L with periodic boundary conditions. The Coulomb energy of the system is

$$E = \sum_{j>i} 1/R(s_i, s_j) \quad (1)$$

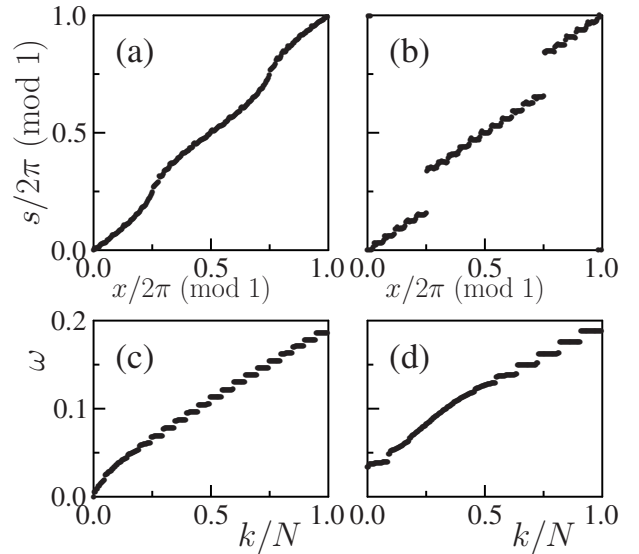


Fig. 2. Hull function $s = h(x)$ (a, b) and phonon spectrum $\omega(k/N)$ (c, d) for incommensurate electron densities $\nu = N/L = 239/233$ (a, c) and $\nu = N/L = 244/233$ (b, d). Here $a = 1.2$ and x gives the positions s_i of electrons at $a = 0$.

where $R(s_i, s_j)$ is the distance between two electrons. We find from geometry $R^2(s_i, s_j) = 4L^2 \sin^2[(s_i - s_j)/2L] + a^2(\sin s_i - \sin s_j)^2$. Here we choose dimensionless units for charge e and length, so that the channel period length is $\ell = 2\pi$ and dimensionless amplitude of channel oscillations is a . We assume an isotropic Coulomb interaction which is justified on small scales where interactions between nearby electrons is dominant. In the limit of large L we have a channel wiggling in (x, z) plane. At $a = 0$ we have electrons on a circle. By definition the parameter a characterizes the nanochannel deformation and we will call it the deformation parameter henceforth.

The equilibrium static configurations are defined by the condition $\partial E/\partial s_i = 0$ with a minimal ground state energy configuration determined numerically by the standard methods [20,23,24]. Using these methods we also find the phonon spectrum $\omega(k)$ of small oscillations at the ground state. It is easy to see that the total energy E is invariant for a homogeneous shift of all electrons by δs when the distance between nearby electrons is $s_{i+1} - s_i = 2\pi m$ that corresponds to electron density $\nu = N/L$ with resonant rational values $\nu_m = 1/m$. Hence, at such a density the Wigner crystal can freely slide along the channel. For irrational density values the properties of sliding are much more tricky. An example is shown in Figure 2 for two very close incommensurate densities ν . For $\nu = 239/233$ we have a smooth hull function $s_i = h(x)(\text{mod } 2\pi)$ with the gapless phonon spectrum $\omega \propto \omega_0 k/N$ at small wave numbers k/N . Here $x = s_i(\text{mod } 2\pi)$ are ground state electron positions s_i at $a = 0$. The dimensional unit of frequency $\omega_0 = (e^2/(m(\ell/2\pi)^3))^{1/2}$ is expressed via the particle charge e , mass m and channel period ℓ , which we omit in the further dimensionless computations. This regime corresponds to the continuous invariant Kolmogorov-Arnold-Moser (KAM) curves as it is

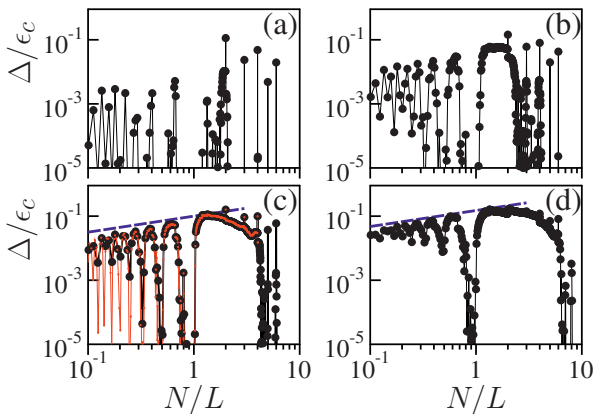


Fig. 3. (Color online) Dependence of the dimensionless phonon gap Δ/ϵ_c on the electron density $\nu = N/L$ for $a = 0.7$ (a), 1 (b), 1.2 (c), 1.5 (d). Here $L = 89$ (black), 233 (gray/red). The straight line shows empirical dependence $\Delta/\epsilon_c \propto (N/L)^{1/2}$ for (c, d), where $\epsilon_c = 2\pi e^2 \nu / \ell = \nu$ is the Coulomb energy.

discussed for the Frenkel-Kontorova model [20–24]. In the KAM regime the invariant curve is analytical and there is no gap in phonon excitations so that the whole chain can slide freely along the nanochannel. This KAM sliding regime is well described in [20–24] where an interested reader can find more details. In contrast, for very close density $\nu = 244/233$ the hull function starts to take the devil’s staircase form, well known for the cantori regime in the Frenkel-Kontorova model. Here, the gap Δ appears in the phonon spectrum so that the crystal is pinned in the channel. This regime corresponds to the insulating phase.

The dependence of phonon gap Δ on electron density ν is shown in Figure 3 for various values of channel deformation amplitude a . At small deformations the gap is zero for a large fraction of densities ν (Fig. 3a) and the crystal can slide freely along the channel. However, at larger deformations the gap disappears only in the vicinity of rational densities ν_m (Figs. 3b, 3c) and at strong deformation regime only narrow zero gap intervals remain around these density values (Fig. 3d). We note that our numerical data are obtained at rather large number of electrons N and channel periods L so that the dependence $\Delta(\nu)$ found numerically corresponds to the limit of infinite channel length. Indeed, the function $\Delta(\nu)$ remains practically unchanged with an increase of L (Fig. 3c). The global dependence of Δ on ν corresponds to frequency of small charge oscillations $\Delta \propto \nu^{3/2} \propto 1/\ell^{3/2}$, being in agreement with data of Figures 3c, 3d.

A remarkable feature of the dependence $\Delta(\nu)$ is its very sharp variation with density ν and deformation a . The dependence is enormously sharp in a vicinity $\nu = 1$: for $\nu < 1$ there is crystal sliding in the channel while only slightly above $\nu = 1$, e.g. for $N/L = 1 + 11/233$, we obtain the insulating phase. This is somewhat similar to a sharp change of conduction properties of organic materials with pressure [14] which effectively modifies ν and a values.

The dependence of phonon gap Δ on channel deformation a is shown in Figure 4 for a few density values ν . The gap changes smoothly with a for $a > a_c$ where a_c is

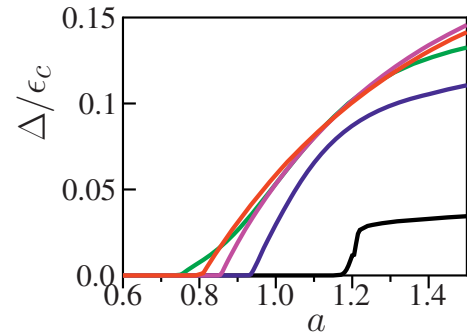


Fig. 4. (Color online) Dependence of rescaled phonon gap Δ/ϵ_c on channel deformation amplitude a at various values of electron density ν with the number of electrons $N = 241$ (black), 269 (blue), 337 (magenta), 377 (red), 307 (green) (curves from right to left at $\Delta/\epsilon_c = 0.01$ respectively) at $L = 233$.

a certain critical value of deformation which depends on density ν . For $a < a_c$ we find very sharp drop of Δ which becomes exponentially small, e.g. Δ drops by 5 orders of magnitude when a decreases by a couple percent in the vicinity of a_c . Since simulations are run at a finite N this means that in the thermodynamic limit $\Delta = 0$ for $a < a_c$. We interpret these data in a way similar to the case of the Frenkel-Kontorova model [21,23,24]: for $a < a_c(\nu)$ we have an analytic invariant KAM curve with a rotation number corresponding to a given density, while for $a > a_c$ this curve is replaced by a cantori with a finite phonon gap and pinning of the crystal.

To better understand the numerical results presented above we derive an approximate dynamical map which determines recursively the electron positions along the channel. The recursion is given by equilibrium conditions $\partial E / \partial s_i = 0$. Assuming that $a \ll 1$ we can expand R in a that, after keeping only nearest electron interactions, gives recursive relations between s_{i-1}, s_i, s_{i+1} . They can be presented in a form of dynamical map

$$\begin{aligned} \bar{v} &= v + 2a^2(1 - \cos \bar{v}) \sin 2\phi, \\ \bar{\phi} &= \phi + \bar{v} + a^2 \sin \bar{v} \cos 2\phi, \end{aligned} \quad (2)$$

where $v = s_i - s_{i-1}$, $\phi = s_i$ are conjugated action-phase variables, bar marks their values after iteration. The map is implicit but symplectic (see e.g. [27]). To check its validity we use the values s_i obtained for the groundstate configuration and extract from them the kick function $g_\phi = \sin 2\phi$ from the values $\bar{v} - v = 2a^2 g_v(v) g_\phi(\phi)$ with $g_v(v) = 1 - \cos v$. Such a check shows that the map (2) indeed gives a good description of actual electron positions s_i up to moderate values of a (Fig. 5).

At small a the phase space of the map is covered by invariant KAM curves as it is shown in Figure 6 (left). At larger a a single chaotic component covers a significant part of the phase space (Fig. 6 right). Locally the dynamics is approximately described by the Chirikov standard map with the chaos parameter $K \approx 4a^2(1 - \cos v)$. According to [22,27] the KAM curves are destroyed at $K > 1$ which is in a good agreement with our numerical

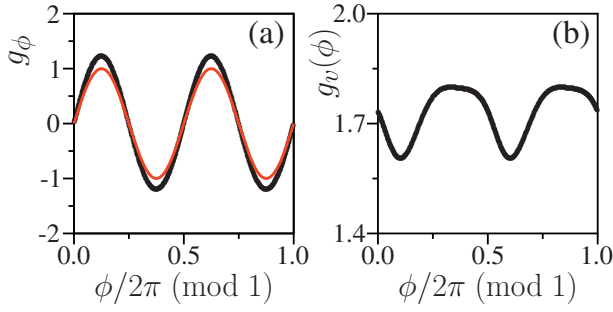


Fig. 5. (Color online) Map kick functions $g_\phi(\phi)$ (a) and $g_v(v)$ (b) obtained from the groundstate electron positions s_i in nanochannel (points), full red/gray curve in (a) shows the theoretical dependence from the map (2), see also text. Here $N = 377$, $L = 233$, $a = 0.5$.

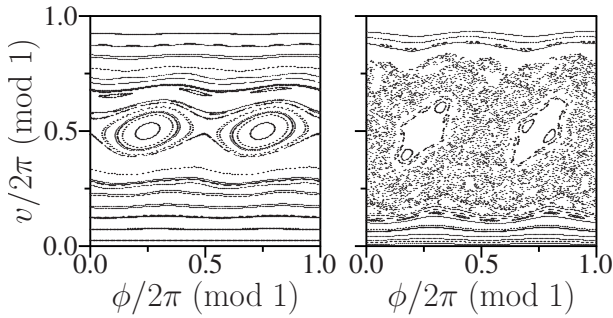


Fig. 6. Poincare section for the dynamical map (2) at $a = 0.25$ (left panel), 0.5 (right panel).

data of Figure 3 where the KAM curve with the golden rotation number $\nu = 0.618\dots$ goes to the cantori regime approximately at $a \approx 0.4$. We note that at small charge density ν the parameter K is small $K \approx 2a^2\nu^2 \ll 1$ that corresponds to the KAM regime and a conducting phase of Wigner crystal in agreement with the data of Figure 3.

We would like to stress that the sliding conditions in the snaked nanochannel are rather different from the cases of the Frenkel-Kontorova model and the Wigner crystal in a periodic potential. Indeed, in these models the particles are pinned for the rational filling values $\nu = N/L = 1/m$ while for the snaked nanochannel we have sliding of the crystal at these ratios.

Of course, the map description is valid only up to moderate a values. At $a > 1$ the expansion in a is no longer valid and explains the asymmetry in the dependence for $\Delta(\nu)$ at $\nu < 1$ and $\nu > 1$ which is absent in the approximate map (2) but is clearly seen in Figure 3. Further studies are required to obtain a map description at large values of deformation a .

3 Discussion

Our studies determined conditions of sliding and pinning of the Wigner crystal in snaked nanochannels. Here, we performed only classical analysis. According to the results of [20] the quantum effects are weak if the dimensionless effective Planck constant $\hbar_{eff} = (2\pi\hbar^2/me^2\ell)^{1/2}$ is small. In fact $\hbar_{eff} \approx (E_k/E_C)^{1/2} \approx 1/r_s^{1/2}$ where E_k , E_C are

electron kinetic and Coulomb energies on a scale ℓ , and $r_s = E_C/E_K$ is given by their ratio. Our studies have been focussed on the regime of small \hbar_{eff} . This is the case for supercapacitors with $\ell/2\pi \sim 1$ nm, large ion mass $m \sim 4 \times 10^4 m_e$ compared to electron mass m_e , that gives $\hbar_{eff} \sim 10^{-3}$.

At present, the experimental results on supercapacitors obtained in [16,17] are not well understood from a theoretical view point. For example, rather opposite theoretical views are given in [18,19,28]. Nanopore materials have wiggling nanochannels and thus we provide first estimates based on the above results obtained for the Wigner snake properties in such a type of channels. Of course, more detailed investigations should be performed in the future. The charge storage process in a supercapacitor starts with small charge density values ν where the ions slide easily in nanochannels since the gap Δ is practically absent there (see Fig. 3). However, with the increase of ν ions form the Wigner crystal which is pinned inside the nanopores at large ν values. We think that this is the physical mechanism behind the charge process of electrochemical capacitors studied in [16,17]. We note that the energy of pinned Wigner crystal can be estimated as $W_W \sim Sde^2/\epsilon(\ell/2\pi)^4$, where S is the surface area, d is the deepness of nanopore layer on the surface and ϵ is the dielectric constant. For typical parameters $\epsilon = 5$, $\ell/2\pi = 1$ nm, $d = 1$ μ m we obtain $W_W/S \approx 5 \times 10^{-3}$ J/cm². It is natural to assume that a part of this energy can be used during the recharging process that makes it comparable with the surface energy density reached in supercapacitors with $W/S \sim 10^{-3}$ J/cm² at maximal capacitance per area $C \approx 400$ μ F/cm² and voltage $U \sim 2$ V [16,17]. We note that our estimate gives an increase of W_W with a decrease of nanopore size ℓ that qualitatively corresponds to the behavior observed experimentally (see e.g. Fig. 3a in [17]). At the above parameters the typical pinning frequency is $\omega_0\Delta/2\pi \sim 50$ GHz so that the Wigner crystal should be sensitive to microwave radiation in this frequency range. Indeed, the experimental studies of CDW in the presence of a RF field show generation of high harmonics in differential resistance [29,30]. We expect that similar effects should be visible for ions in nanopore materials. We also note that recent experimental I - V -curves obtained for large radius ions in sub-nanometer carbon pores have negative I - V slopes at certain voltages that may be a first indication of ion crystal pinning in nanopores (see Fig. 6 in [31]).

In contrast, for CDW in organic conductors [14] we have $m \sim m_e$, $\ell/2\pi \sim 3$ Å that gives $\hbar_{eff} \sim 0.5$ so that quantum effects can play an important role. Further studies are required to analyze quantum properties of crystal sliding but we expect that they will have similarities with the quantum Wigner crystal in a periodic potential [20] and the quantum Frenkel-Kontorova model [25]. The classical pinned phase should correspond to the insulator phase, while we expect that the classical sliding phase may correspond to the superconducting regime in the quantum case. Indeed, the sliding phase has a linear dispersion law $\omega(k)$ that can be similar to the situation

in the superfluid phase. The sharp transitions from conducting to insulating phase with charge density variation are well pronounced in the classical regime and are expected to be present also in the quantum case. Such a sharp density variation of conducting properties, found in our model, can be linked to a high sensitivity of conductivity of organic conductors to pressure found in experiments. Further studies should provide more insight into the quantum properties of Wigner crystal in snaked nanochannels and organic molecular chains. It would be very interesting to study such effects by experimentally creating artificial snaked channels with electrons on a surface of liquid helium using the methods discussed in [11,32]. At present, the experimental technology developed for electrons on liquid helium surface allow move electrons one by one along artificial straight channels created electrostatically [11,32]. Another possibility can be two-dimensional electron gas in antidot arrays similar to those studied in [33] where at low electron density it is possible to have about one electron per lattice cell with important influence of Coulomb interactions on electron transport.

We thank P. Simon and P.L. Taberna for useful discussions and pointing to us results presented in [31]. This research is supported in part by the ANR PNANO project NANOTERRA.

References

1. E. Wigner, Phys. Rev. **46**, 1002 (1934)
2. J.S. Meyer, K.A. Matveev, J. Phys. C.: Condens. Matter **21**, 023203 (2009)
3. Y. Monarkha, K. Kono, *Two-Dimensional Coulomb Liquids and Solids* (Springer-Verlag, Berlin, 2004)
4. D.H.E. Dubin, T.M. O'Neil, Rev. Mod. Phys. **71**, 87 (1999)
5. V.E. Fortov, A.V. Ivlev, S.A. Khrapak, A.G. Khrapak, G.E. Morfill, Phys. Rep. **421**, 1 (2005)
6. O.M. Auslaender, H. Steinberg, A. Yacoby, Y. Tserkovnyak, B.I. Halperin, K.W. Baldwin, L.N. Pfeiffer, K.W. West, Science **308**, 88 (2005)
7. V.V. Deshpande, B. Chandra, R. Caldwell, D.S. Novikov, J. Hone, M. Bockrath, Science **323**, 106 (2009)
8. Y. Jompol, C.J.B. Ford, J.P. Griffiths, I. Farrer, G.A. Jones, D. Anderson, D.A. Ritchie, T.W. Silk, A.J. Schofield, Science **325**, 597 (2009)
9. V.V. Deshpande, M. Bockrath, L.I. Glazman, A. Yacoby, Nature **464**, 209 (2010)
10. L.H. Kristinsdóttir, J.C. Cremon, H.A. Nilsson, H.Q. Xu, L. Samuelson, H. Linke, A. Wacker, S.M. Reimann, Phys. Rev. B **83**, R041101 (2011)
11. D.G. Rees, I. Kuroda, C.A. Marrache-Kikuchi, M. Höfer, P. Leiderer, K. Kono, Phys. Rev. Lett. **106**, 026803 (2011)
12. W.A. Little, Phys. Rev. A **134**, 1416 (1964)
13. W.A. Little, Sci. Am. **212**, 21 (1965)
14. D. Jérôme, Historical Approach to Organic Superconductivity, in *The Physics of Organic Superconductors and Conductors*, edited by A. Lebed (Springer-Verlag, Berlin, 2008), p. 3
15. R.E. Thorne, Phys. Today **5**, 43 (1996)
16. P. Simon, Y. Gogotsi, Nature Mater. **7**, 845 (2008)
17. P. Simon, Y. Gogotsi, Phil. Trans. R. Soc. A **368**, 3457 (2010)
18. B. Skinner, M.S. Loth, B.I. Shklovskii, Phys. Rev. Lett. **104**, 128302 (2010)
19. B. Skinner, T. Chen, M.S. Loth, B.I. Shklovskii, Phys. Rev. E **83**, 056102 (2011)
20. I. Garcia-Mata, O.V. Zhirov, D.L. Shepelyansky, Eur. Phys. J. B **41**, 325 (2007)
21. O.M. Braun, Yu.S. Kivshar, *The Frenkel-Kontorova Model: Concepts, Methods, Applications* (Springer-Verlag, Berlin, 2004)
22. B.V. Chirikov, Phys. Rep. **52**, 263 (1979)
23. S. Aubry, Physica D **7**, 240 (1983)
24. O.V. Zhirov, G. Casati, D.L. Shepelyansky, Phys. Rev. E **65**, 026220 (2002)
25. O.V. Zhirov, G. Casati, D.L. Shepelyansky, Phys. Rev. E **67**, 056209 (2003)
26. M. Mézard, G. Parisi, M.A. Virasoro, *Spin Glass Theory and Beyond* (World Sci., Singapore, 1987)
27. A.J. Lichtenberg, M.A. Lieberman, *Regular and chaotic dynamics* (Springer, Berlin, 1992)
28. A.L. Efros, arXiv:1103.3878 (2011)
29. P. Monceau, J. Richard, M. Renard, Phys. Rev. Lett. **45**, 43 (1980)
30. P. Monceau, Historical Approach to Organic Superconductivity, in *The Physics of Organic Superconductors and Conductors*, edited by A. Lebed (Springer-Verlag, Berlin, 2008), p. 17
31. R. Lin, P. Huang, J. Ségalini, C. Largeot, P.I. Taberna, J. Chmiola, Y. Gogotsi, P. Simon, Electrochimica Acta **54**, 7025 (2009)
32. E. Rousseau, D. Ponarín, L. Hristakos, O. Avenel, E. Varoquaux, Y. Mukharsky, Phys. Rev. B **79**, 045406 (2009)
33. M.V. Budantsev, Z.D. Kvon, A.G. Pogosov, G.M. Gusev, J.C. Portal, D.K. Maude, N.T. Moshegov, A.I. Toropov, Physica B **256-258**, 595 (1998)